Science Advances
AAAS

advances.sciencemag.org/cgi/content/full/6/11/eaay2732/DC1

Supplementary Materials for

Magnetar formation through a convective dynamo in protoneutron stars

Raphaël Raynaud*, Jérôme Guilet, Hans-Thomas Janka, Thomas Gastine

*Corresponding author. Email: raphael.raynaud@cea.fr

Published 13 March 2020, *Sci. Adv.* **6**, eaay2732 (2020)
DOI: 10.1126/sciadv.aay2732

This PDF file includes:

Supplementary Materials

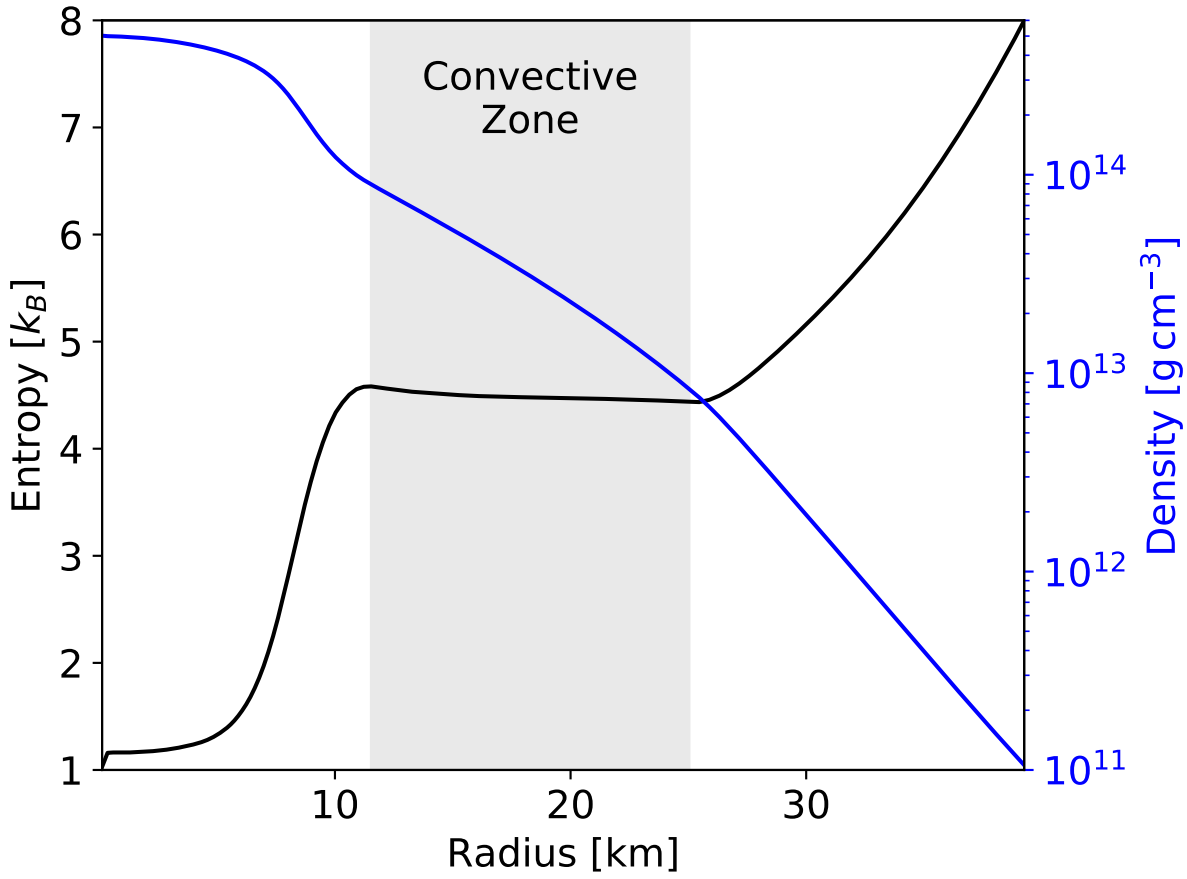

Fig. S1. Entropy per baryon and density profile inside the PNS 0.2 s after bounce. The entropy per baryon is expressed in units of the Boltzmann constant. The shaded region highlights the convective zone according to the Schwarzschild criterion $dS/dr \leq 0$. Note that the convective zone appears almost isentropic.

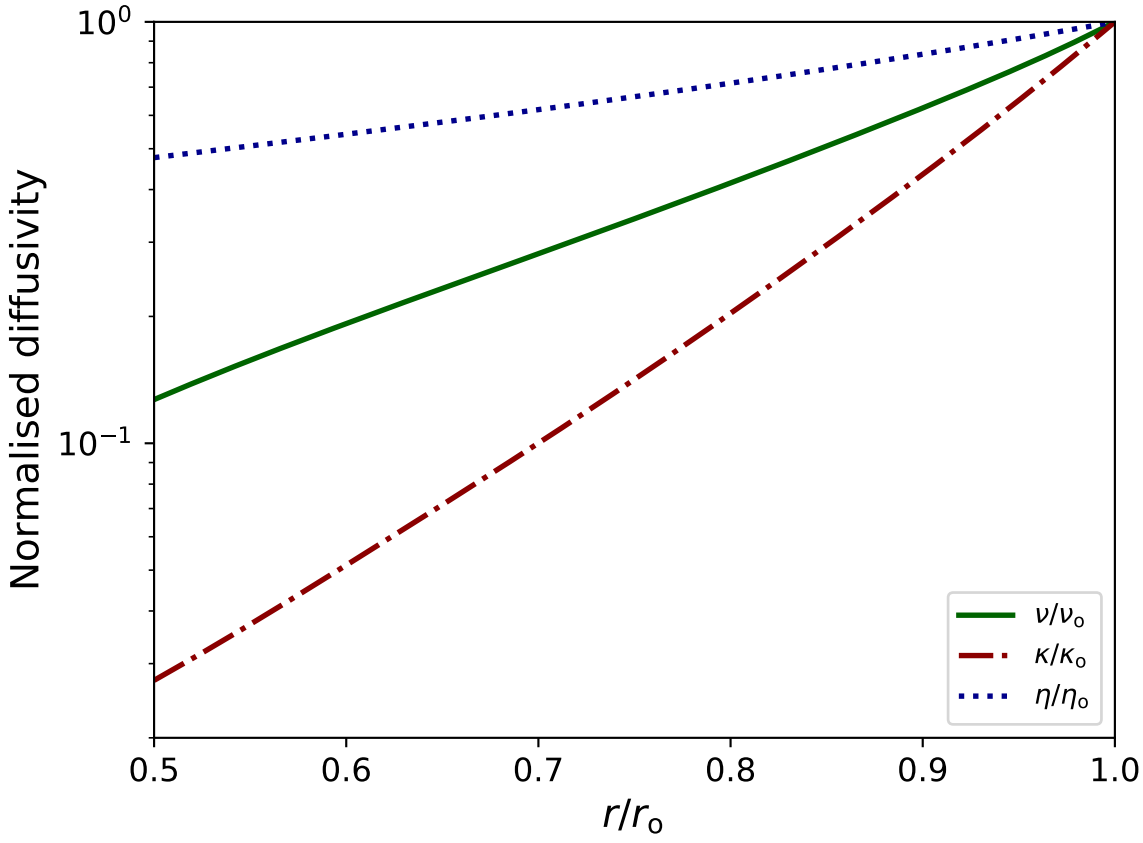

Fig. S2. Normalized diffusivity profiles as a function of radius. The convective zone extends up to $r_o = 25$ km. For the model diplayed in Fig. 1, the top values of the diffusivities are $\nu_o = 4.67 \times 10^{12}\,\mathrm{cm}^2/\mathrm{s}$, $\kappa_o = 4.67 \times 10^{13}\,\mathrm{cm}^2/\mathrm{s}$ and $\eta_o = 2.33 \times 10^{12}\,\mathrm{cm}^2/\mathrm{s}$. From the 1D model, we derive realistic estimates $\nu_o = 2.37 \times 10^{10}\,\mathrm{cm}^2/\mathrm{s}$, $\kappa_o = 3.16 \times 10^{12}\,\mathrm{cm}^2/\mathrm{s}$ and $\eta_o = 8.87 \times 10^{-5}\,\mathrm{cm}^2/\mathrm{s}$.

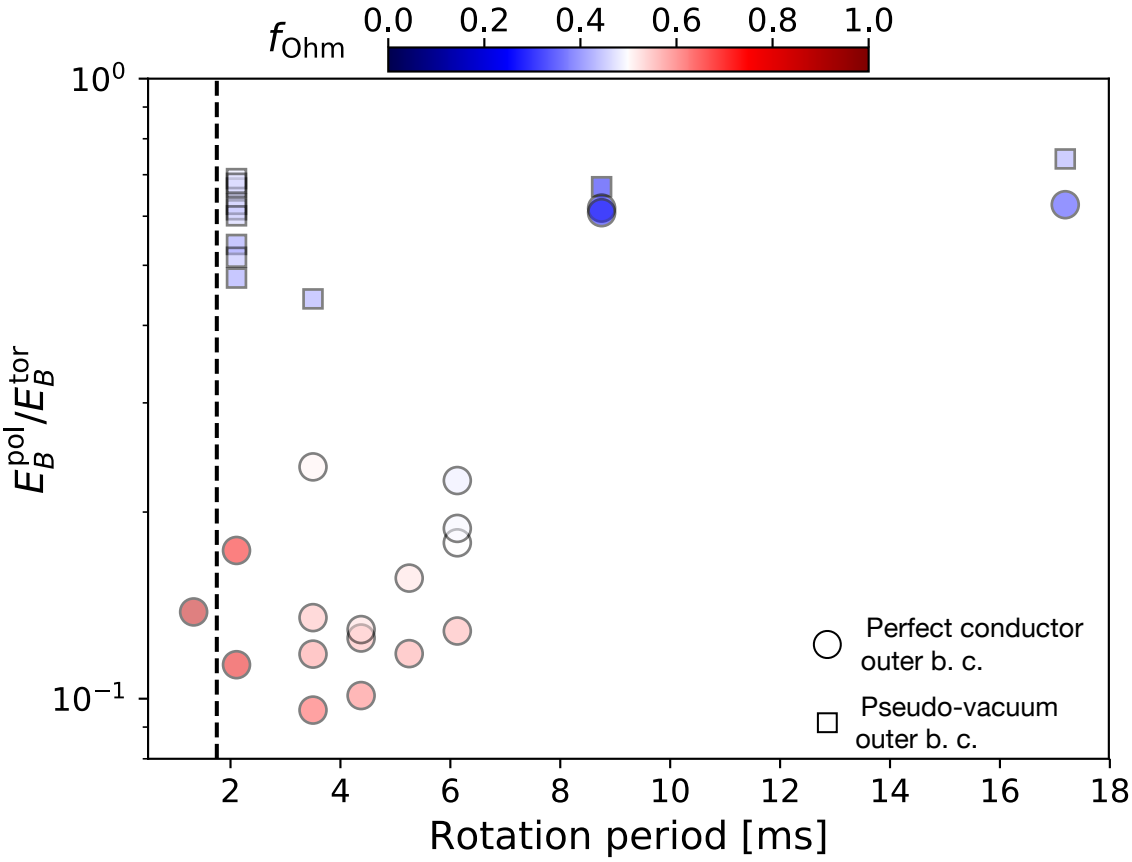

Fig. S3. Ratio of the poloidal and toroidal magnetic energy.

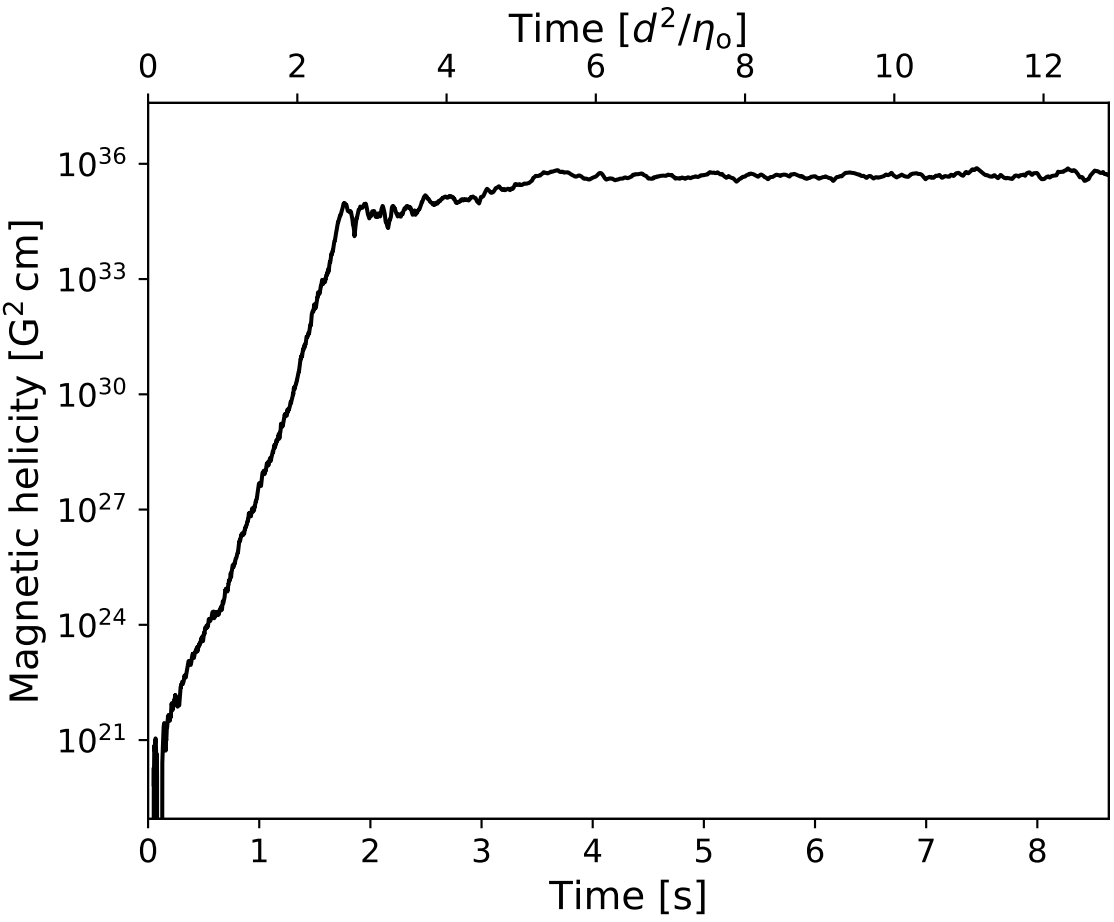

Fig. S4. Time evolution of the magnetic helicity for a run that saturates on the strong field branch with *P* = 2.1 s and Pm = 2. The volume averaged magnetic helicity is $H = \frac{1}{V}\int_V \mathbf{A}\cdot\mathbf{B}$, where we define the magnetic vector potential $\mathbf{A} = \nabla \times B_P\mathbf{e}_r + B_T\mathbf{e}_r$, with B_P and B_T the magnetic poloidal and toroidal scalar potentials. This definition amounts to the gauge fixing condition $\partial_\theta(\sin\theta A_\theta) + \partial_\phi A_\phi = 0$. The upper x-axis is labelled in units of the magnetic diffusion time.

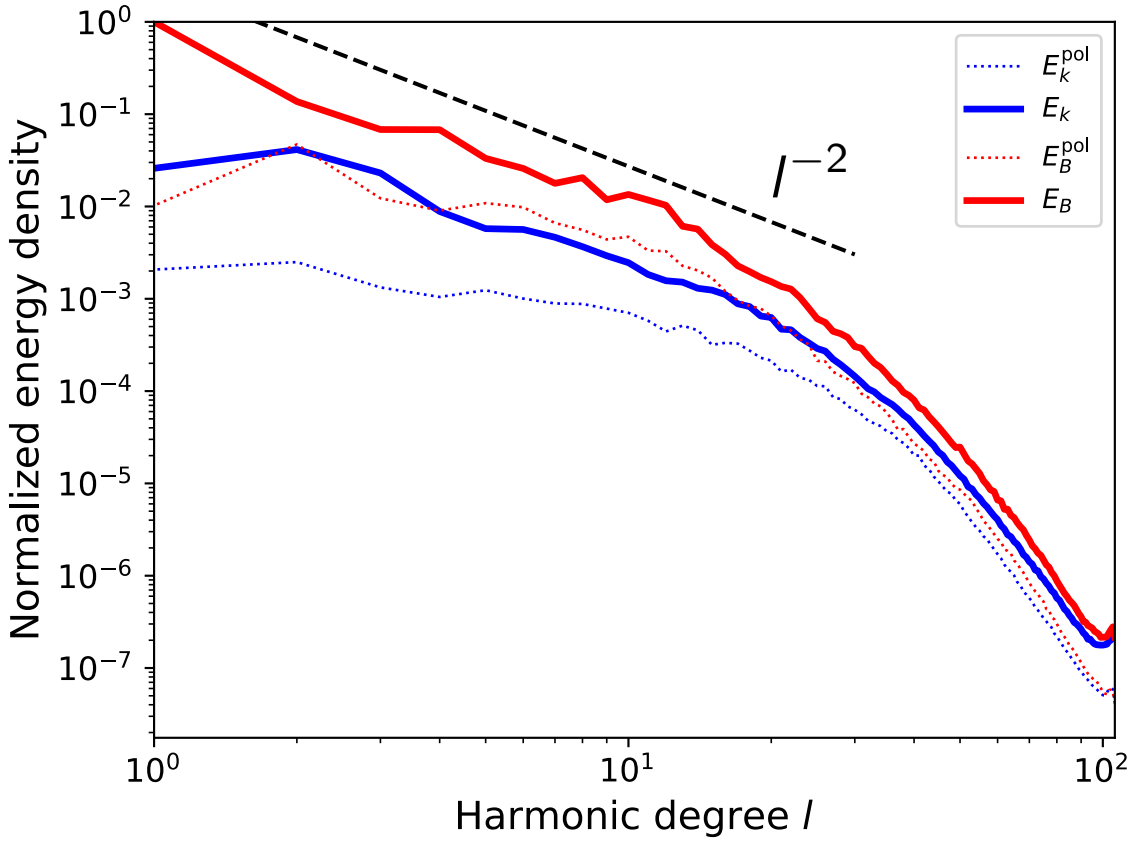

Fig. S5. Kinetic (blue) and magnetic (red) energy spectra. The dotted lines show the poloidal component. This spectrum is taken in the saturated state of the model displayed in Fig. 1. The dashed line gives the eye an indicative slope.

Table S1. Overview of the numerical simulations carried out. For all models, $Pr = 0.1$ and the shell aspect ratio $\chi = r_\mathrm{i}/r_\mathrm{o} = 0.5$. $V_\mathrm{bc} = \{1, 2\}$ stands for stress-free or no-slip mechanical boundary conditions, respectively. $B_\mathrm{bc} = \{2, 4\}$ stands for perfect-conductor or pseudo-vacuum outer magnetic boundary condition, respectively.

V_bc	B_bc	P [ms]	E	Pm	Ra	B_dip [G]	$B_\mathrm{tor}^\mathrm{axi}$ [G]	Ro	E_B/E_K	$E_B^\mathrm{pol}/E_B^\mathrm{tor}$	f_Ohm	N_r	N_ϕ
1	2	1.3	5.000×10^{-4}	2	1.2×10^{4}	1.2×10^{15}	7.6×10^{15}	2.1×10^{-2}	2.5×10^{1}	0.138	0.873	145	320
1	4	2.1	1.000×10^{-3}	2	5.9×10^{3}	3.8×10^{14}	8.8×10^{14}	3.5×10^{-2}	5.9×10^{-1}	0.477	0.391	145	320
1	2	2.1	1.000×10^{-3}	2	5.9×10^{3}	8.7×10^{14}	6.9×10^{15}	4.0×10^{-2}	1.2×10^{1}	0.113	0.797	145	320
1	4	2.1	1.000×10^{-3}	3	5.9×10^{3}	3.3×10^{14}	7.5×10^{14}	3.4×10^{-2}	6.6×10^{-1}	0.540	0.393	145	320
1	4	2.1	1.000×10^{-3}	3	5.9×10^{3}	3.6×10^{14}	8.0×10^{14}	3.3×10^{-2}	8.0×10^{-1}	0.515	0.425	145	320
1	2	2.1	1.000×10^{-3}	3	5.9×10^{3}	1.3×10^{15}	6.1×10^{15}	4.0×10^{-2}	1.3×10^{1}	0.173	0.764	145	320
1	4	2.1	1.000×10^{-3}	5	5.9×10^{3}	3.6×10^{14}	6.3×10^{14}	2.9×10^{-2}	1.1×10^{0}	0.615	0.456	145	320
1	4	2.1	1.000×10^{-3}	5	5.9×10^{3}	3.3×10^{14}	6.4×10^{14}	3.0×10^{-2}	1.0×10^{0}	0.601	0.448	145	320
1	4	2.1	1.000×10^{-3}	10	5.9×10^{3}	2.5×10^{14}	4.6×10^{14}	2.9×10^{-2}	1.2×10^{0}	0.627	0.449	193	320
1	4	2.1	1.000×10^{-3}	10	5.9×10^{3}	3.0×10^{14}	5.0×10^{14}	2.8×10^{-2}	1.3×10^{0}	0.666	0.451	145	320
1	4	2.1	1.000×10^{-3}	20	5.9×10^{3}	2.5×10^{14}	4.7×10^{14}	2.7×10^{-2}	1.8×10^{0}	0.690	0.476	257	1024
1	4	2.1	1.000×10^{-3}	40	5.9×10^{3}	1.5×10^{14}	3.6×10^{14}	2.7×10^{-2}	1.8×10^{0}	0.678	0.458	257	1024
1	2	3.5	1.660×10^{-3}	2	5.9×10^{3}	7.1×10^{14}	6.6×10^{15}	8.9×10^{-2}	5.6×10^{0}	0.096	0.682	145	320
1	4	3.5	1.660×10^{-3}	5	5.9×10^{3}	2.5×10^{14}	9.5×10^{14}	9.3×10^{-2}	4.1×10^{-1}	0.441	0.401	145	320
2	2	3.5	1.660×10^{-3}	5	5.9×10^{3}	8.1×10^{14}	4.5×10^{15}	7.2×10^{-2}	4.3×10^{0}	0.237	0.512	257	864
1	2	3.5	1.660×10^{-3}	5	5.9×10^{3}	8.6×10^{14}	6.8×10^{15}	9.1×10^{-2}	6.3×10^{0}	0.118	0.607	181	512
1	2	3.5	1.660×10^{-3}	7	5.9×10^{3}	8.2×10^{14}	6.2×10^{15}	9.1×10^{-2}	5.3×10^{0}	0.135	0.574	161	512
1	2	4.4	2.075×10^{-3}	2	5.9×10^{3}	6.6×10^{14}	5.9×10^{15}	1.2×10^{-1}	4.1×10^{0}	0.101	0.640	161	512
1	2	4.4	2.075×10^{-3}	5	5.9×10^{3}	7.9×10^{14}	6.1×10^{15}	1.3×10^{-1}	4.1×10^{0}	0.125	0.575	161	512
1	2	4.4	2.075×10^{-3}	7	5.9×10^{3}	7.3×10^{14}	6.1×10^{15}	1.3×10^{-1}	3.9×10^{0}	0.129	0.536	161	512
1	2	5.3	2.490×10^{-3}	2	5.9×10^{3}	6.7×10^{14}	5.1×10^{15}	1.5×10^{-1}	2.8×10^{0}	0.118	0.597	193	512
1	2	5.3	2.490×10^{-3}	5	5.9×10^{3}	6.2×10^{14}	4.8×10^{15}	1.5×10^{-1}	2.7×10^{0}	0.156	0.533	201	864
1	2	6.1	2.905×10^{-3}	2	5.9×10^{3}	6.7×10^{14}	5.0×10^{15}	1.9×10^{-1}	2.4×10^{0}	0.129	0.583	201	864
1	2	6.1	2.905×10^{-3}	5	5.9×10^{3}	6.0×10^{14}	4.0×10^{15}	1.8×10^{-1}	1.9×10^{0}	0.178	0.503	201	864
1	2	6.1	2.905×10^{-3}	5	5.9×10^{3}	5.2×10^{14}	3.9×10^{15}	1.9×10^{-1}	1.6×10^{0}	0.188	0.491	201	864
1	2	6.1	2.905×10^{-3}	7	5.9×10^{3}	5.1×10^{14}	3.4×10^{15}	1.8×10^{-1}	1.5×10^{0}	0.225	0.479	201	864
1	4	8.8	4.150×10^{-3}	5	5.9×10^{3}	1.2×10^{14}	2.6×10^{14}	3.0×10^{-1}	1.2×10^{-1}	0.669	0.242	145	320
2	2	8.8	4.150×10^{-3}	5	5.9×10^{3}	2.2×10^{14}	6.1×10^{14}	2.6×10^{-1}	2.2×10^{-1}	0.608	0.242	145	320
2	2	8.8	4.150×10^{-3}	5	5.9×10^{3}	2.3×10^{14}	6.2×10^{14}	2.5×10^{-1}	2.5×10^{-1}	0.618	0.258	257	864
1	2	17.2	8.150×10^{-3}	5	5.9×10^{3}	1.5×10^{14}	3.3×10^{14}	7.6×10^{-1}	9.9×10^{-2}	0.626	0.292	145	320
1	4	17.2	8.150×10^{-3}	5	5.9×10^{3}	3.1×10^{14}	6.0×10^{14}	7.1×10^{-1}	2.3×10^{-1}	0.742	0.403	181	640